Evidence for a Monomeric Structure of Nonribosomal Peptide Synthetases

Stephan A. Sieber,[1,2,4] Uwe Linne,[1,4]
Nathan J. Hillson,[2] Eric Roche,[2]
Christopher T. Walsh,[2]
and Mohamed A. Marahiel[1,3]
[1]Biochemie/Fachbereich Chemie
Philipps-Universität Marburg
Hans-Meerwein-Straße
35032 Marburg
Germany
[2]Department of Biological Chemistry
and Molecular Pharmacology
Harvard Medical School
Boston, Massachusetts 02115

Summary

Nonribosomal peptide synthetases (NRPS) are multi-modular biocatalysts that bacteria and fungi use to assemble many complex peptides with broad biological activities. The same modular enzymatic assembly line principles are found in fatty acid synthases (FAS), polyketide synthases (PKS), and most recently in hybrid NRPS/PKS multienzymes. FAS as well as PKS are known to function as homodimeric enzyme complexes, raising the question of whether NRPS may also act as homodimers. To test this hypothesis, biophysical methods (size exclusion chromatography, analytical equilibrium ultracentrifugation, and chemical cross-linking) and biochemical methods (two-affinity-tag-system and complementation studies with enzymes being inactivated in different catalytic domains) were applied to NRPS subunits from the gramicidin S (GrsA-ATE), tyrocidine (TycB$_1$-CAT and TycB$_{2-3}$-AT.CATE), and enterobactin (EntF-CATTe) biosynthetic systems. These methods had revealed the dimeric structure of FAS and PKS previously, but all three NRPS systems investigated are functionally active as monomers.

Introduction

Multimodular nonribosomal peptide synthetases (NRPS) from bacteria and fungi are involved in the synthesis of many biologically active peptides. These compounds display antibiotic, cytostatic, or immuno-suppressive characteristics (e.g., tyrocidine, penicillin, cephalosporin, vancomycin, and cyclosporin) and feature a great chemical and structural diversity [1–3]. Another important class of diverse natural-product-generating enzymes are polyketide synthases (PKS), which have a multimodular architecture similar to NRPS. NRPS-PKS hybrid enzymes are also well known in nature. Because of their potential to produce pharmaceutically interesting agents like epothilone, a potent anticancer agent, these hybrid enzymes are of outstanding interest [4–6].

Each module within a NRPS enzyme is outfitted with the necessary catalytic units for incorporation of an amino acid into the product. The total number of modules corresponds to the number of incorporated residues, and the peptide synthesis takes place colinear to the enzymatic template [7, 8]. Each module consists of several distinct domains performing the various catalytic activities. The substrate is first specifically recognized and activated by an adenylation domain (A domain) through the hydrolysis of ATP [9]. Subsequently, the resulting aminoacyl adenylate is tethered onto the 4′-phosphopantetheine cofactor of the peptidyl carrier protein (PCP) by the formation of a thioester bond [10]. In this tethered state, the substrate can be modified by epimerization (E domain) [11], N-methylation (M domain) [12], and heterocyclization (Cy domain) [13] domains. These reactions significantly contribute to the structural diversity of the products [2]. Peptide bond formation is catalyzed by the condensation domain (C domain) or Cy domain. The C domain catalyzes the acyl transfer by the nucleophilic attack of the amino acid bound on the C-terminal PCP on the activated thioester bond of the N-terminal PCP bearing the growing chain [14, 15]. The result of this elongation reaction is a regenerated cofactor of the N-terminal PCP and an extended peptide chain bound to the C-terminal PCP. In many NRPS, the final product is released through hydrolysis or cyclization by a C-terminal thioesterase domain (Te domain) of the termination module, resulting in linear, branched-cyclic, or cyclic peptides and regenerating the enzyme for a new catalytic cycle [16].

Fatty acid synthases (FAS) and polyketide synthases use an equivalent assembly-line strategy with multidomain modules for monomeric acyl-CoA incorporated and elongated. The acyl chains in each module are tethered as thioesters to phosphopantetheinylated carrier protein domains. This is the same logic of a cascade of elongating acyl-S-pant-carrier protein intermediates utilized by the NRPS enzymatic machinery [17].

Many enzymes catalyzing sequential metabolic reactions aggregate by noncovalent linking of identical or nonidentical subunits to form multienzyme complexes. The fatty acid synthases of eucaryotes are examples of an enzyme complex composed of two identical subunits (Figure 1) [18]. Various investigations have unequivocally revealed the dimeric organization of multimodular polyketide synthases [19, 20]. The existence of NRPS-PKS hybrid enzymes in nature is well known [21–23], and it would be useful to know if NRPS modules that interface with dimeric PKS modules are themselves monomeric or oligomeric. The oligomeric state of NRPS enzymatic machinery is unknown. Knowledge of the quaternary structure of NRPS, defined as the spatial geometry of two identical neighboring subunits, is not only important for understanding reactions occurring on or between enzymes, but may also be useful for engineering new hybrid enzymes by swapping modules or domains.

Although structures are now known for individual domains [9, 10, 24, 25], no high-resolution structure is

[3]Correspondence: marahiel@chemie.uni-marburg.de
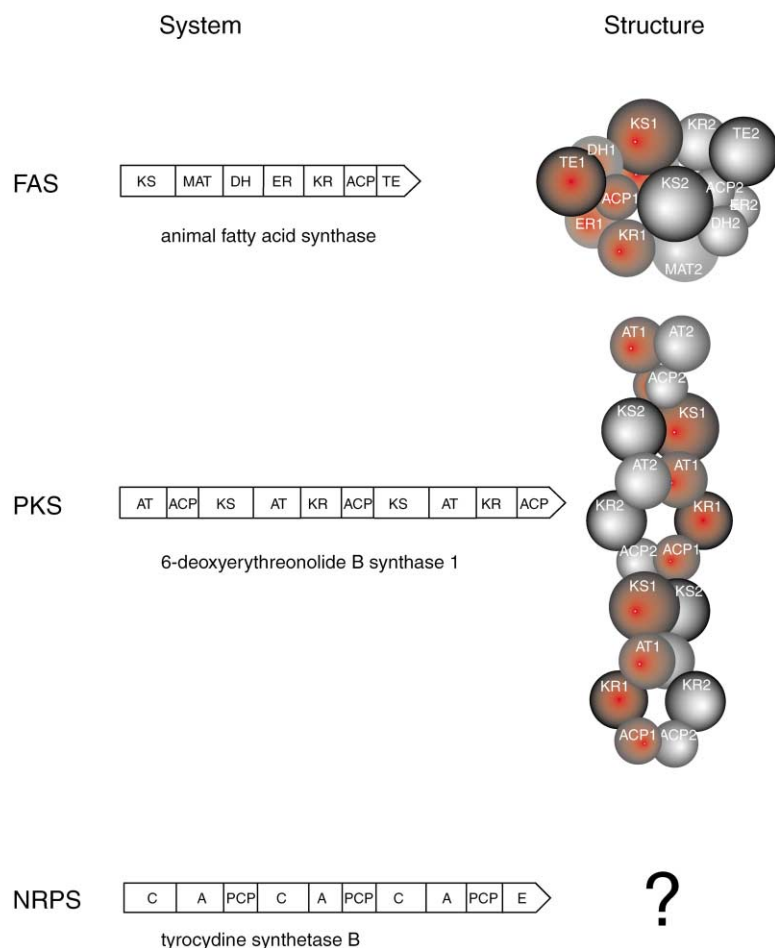[4]These authors contributed equally to this work.

System

Structure

FAS

| KS | MAT | DH | ER | KR | ACP | TE |

animal fatty acid synthase

PKS

| AT | ACP | KS | AT | KR | ACP | KS | AT | KR | ACP |

6-deoxyerythronolide B synthase 1

NRPS

| C | A | PCP | C | A | PCP | C | A | PCP | E |

tyrocydine synthetase B

?

available for a multidomain NRPS or PKS. Therefore, PKS and FAS enzymes were previously characterized by gel filtration, ultracentrifugation, and chemical cross-linking experiments to ascertain oligomerization state of functional enzymes [20, 26, 27].

The topology of FAS and PKS enzymes has been additionally investigated by an in vitro complementation strategy. Site-directed mutagenesis was applied to produce genetically modified enzymes specifically inactivated in one domain. On inactivation of the ketosynthase (KS, carbon-carbon bond forming activity) or acyl carrier protein (ACP, homologous to NRPS PCP domains), all homodimeric enzymes lost their ability for product synthesis. An exchange of subunits from two differently mutated homodimeric enzymes generated a heterodimer carrying both (KS and ACP) mutations in opposite subunits. This heterodimer retains catalytic activity by cooperation of the remaining active KS and ACP domains across both subunits. The functional interaction between KS and ACP from opposite subunits in a dimer has also been supported by crosslinking. This postulated mechanism has been shown for both PKS and FAS through product formation catalyzed by a heterodimer [18, 19, 28, 29].

Based on these results, a double-helical structure model for modular PKS was proposed [20]. According to this model, the enzyme subunits are orientated head-

to-head and folded in an interwound helical manner. KS, ACP, and AT domains are building the core, which is necessary for the observed interaction between KS and ACP domains from different strands (Figure 1). Optional domains like the KR domain are accommodated in outside loops. The model for FAS enzymes considers also functional interactions within each of the two subunits that have been observed by crosslinking studies [30, 31].

Despite many analogies in the organization and reaction mechanism, in contrast to FAS and PKS little is known about the quaternary structure of NRPS. Mainly gel filtration experiments are mentioned in literature, e.g., the molecular weight of the enzymes EntB, EntE, and EntF of the enterobactin synthetase were determined to be monomeric for EntE and EntF and trimeric for EntB [32]. Other NRPS enzymes, like the δ-(L-α-aminoadipyl)-L-cysteinyl-D-valine synthetase as well as the pipecolate-incorporating enzyme for the biosynthesis of rapamycin, also showed a monomeric behavior on gel filtration [33, 34]. The objective of our research efforts was therefore to explore the quaternary structure of NRPS with similar strategies to those which have been successfully applied to discover the structure of PKS and FAS. Investigations were carried out with several representative NRPS systems different in size and assembly-line organization: GrsA (domains ATE) [14], $TycB_1$ (domains CAT) [35], the dimodular enzyme $TycB_{2-3}$

Table 1. Results of Size Exclusion Chromatography

Enzyme	Theoretical Mass m_t (kDa)	Obtained Mass m_o (kDa)	Quotient m_o/m_t
GrsA	127	167	1,31
ProCAT	119	162	1,36
TycB$_{2-3}$	237	364	1,53
HMWP1	350	721; 424	2.06; 1.21

The table shows the theoretical (m_t) and obtained (m_o) molecular weights of all four applied proteins gained under the conditions as described in Experimental Procedures. The quotient m_o/m_t is a measure of how much the obtained weight exceeds the theoretical monomeric weight of the proteins (a value of 1 is obtained for monomers and a value of 2 for dimers).

(domains AT.CATE) [36], and EntF (domains CATTe) [32, 37]. Our results indicate monomeric behavior of these NRPS enzyme subunits.

Results

The first part of the strategy focused on the chemical and biophysical properties of the enzymes. Gel filtration, ultracentrifugation, and crosslinking are applicable methods to gain general information about size and molecular weight of a protein. The second part investigated the functional complementation between subunits carrying inactivated domains, which would additionally give a biochemical proof of a dimeric structure. In order to complete the biochemical part of the strategy, we constructed enzymes with two different affinity tags. Only a putative heterodimer with two different tags should be able to bind to two successive affinity columns. All enzymes were proven to be active by ATP-PP$_i$ exchange and by aminoacylation studies prior to their use.

Gel Filtration, Chemical Crosslinking, and Equilibrium Analytical Ultracentrifugation

First attempts to elucidate the quaternary structure of NRPS modules were carried out utilizing gel filtration experiments (Table 1; for experimental details see Experimental Procedures). Each NRPS enzyme, GrsA (127 kDa), TycB$_1$ (119 kDa), and TycB$_{2-3}$ (237 kDa), eluted with an apparent monomeric weight. No protein elution at a corresponding dimeric or higher mass was observed. In contrast, gel filtration of the mixed NRPS-PKS hybrid enzyme HMWP1 (350 kDa) carried out under the same conditions revealed significant formation of a monomer (424 kDa) and an additional elution peak of a protein with the approximate weight of a dimer (721 kDa).

Bifunctional crosslinking reagents such as 1,3-dibromopropanone (DBP) and bismaleimidohexane (BMH) have been shown to crosslink PKS modules as homodimers [20, 38]. DBP and BMH covalently connect thiol groups within a distance of 5 Å and 16 Å, respectively. We applied the same crosslinking experiments to these NRPS modules. The molecular weights of any crosslinked proteins were investigated using SDS-PAGE and MALDI-TOF mass spectrometry. To avoid nonspecific linkages, the crosslinkers were used only up to a 3- to 10-fold molar excess according to the manufacturer's protocol (ICN, Pierce). After incubation with BMH, the

electrophoretic mobilities of GrsA and TycB$_1$ proteins decreased marginally, resulting in a shift to higher molecular weights (from ~120 kDa to ~140–160 kDa) on SDS gels, whereas in the case of DBP no change of migration was observed (Figure 2). On the basis of these results, there is no indication for the existence of a dimer, since the electrophoretic mobilities of the new bands (~140–160 kDa) are in between the monomeric (~120 kDa) and dimeric weight (~240 kDa) of GrsA and TycB$_1$. Similar results were obtained for the larger dimodular enzyme TycB$_{2-3}$ (237 kDa), which revealed one new protein band after reaction with both BMH and DBP, corresponding to an electrophoretic mobility of a protein of ~290 kDa (Figure 2). The determination of the electrophoretic mobility of the new protein band was carried out in direct comparison with a parallel crosslinking of phosphorylase b (97-582 kDa) [38]. Again, for the larger dimodular enzyme the electrophoretic mobility of the new protein band does not represent a dimer (474 kDa). Analogous experiments were carried out with dimethyl suberimidate (DMS), a crosslinker which connects primary amines in a distance of about 11 Å. None of these crosslinking reactions revealed altered protein patterns on SDS gels (data not shown). The crosslinking results were confirmed by application of MALDI-TOF mass spectrometry. Direct comparison of crosslinker treated and untreated samples revealed neither peaks for GrsA and TycB$_1$ corresponding to the singly charged molecular ions (~250 kDa) nor to odd multiply charged species (M^{3+} ~85 kDa and M^{5+} ~50 kDa) of the dimers (MALDI-TOF spectra of GrsA are shown in Figures 2D and 2E). The differences of the molecular masses of treated and untreated samples observed were "only" ~1500 Da for TycB$_1$ and ~600 Da for GrsA larger than the monomer molecular weights, indicating the reaction of five and two molecules of BMH (276 Da), respectively. TycB$_{2-3}$ was too large for MALDI-TOF investigations.

Analytical ultracentrifugation was applied to determine the native molecular weight for the dimodular enzyme fragment TycB$_{2-3}$ and the monomodular enzyme EntF.

To establish the association properties of TycB$_{2-3}$, sedimentation equilibrium experiments were conducted at several protein concentrations (Figure 3). For the global equilibrium analysis, eight scans (Figure 3A) of speeds ranging from 5,000 to 12,500 rpm and 0.39 and 0.57 O.D. loading concentrations were fit to a monomer-dimer model. Monomer molecular weight and the association constant were floated global parameters and were forced to be the same for all the included data sets. The system could be well described with this monomer-dimer model, which resulted in random residuals (Figure 3B) and a monomer molecular weight of 238.07 ± 18.21 kDa (Figure 3C), which is in agreement with the protein sequence predicted molecular weight (237.69 kDa). The dissociation constant of 3.489 ± 0.186 μM suggests the presence of dimer only at high concentrations, which were required for ultracentrifugation experiments (Figure 3D).

Sedimentation equilibrium analysis of EntF was conducted at a single protein concentration (Figures 3E and 3F). For the global equilibrium analysis, four scans (Figure 3E) of speeds ranging from 8,000 to 17,000 rpm

A GrsA (127 kDa)

B TycB₁ (119 kDa)
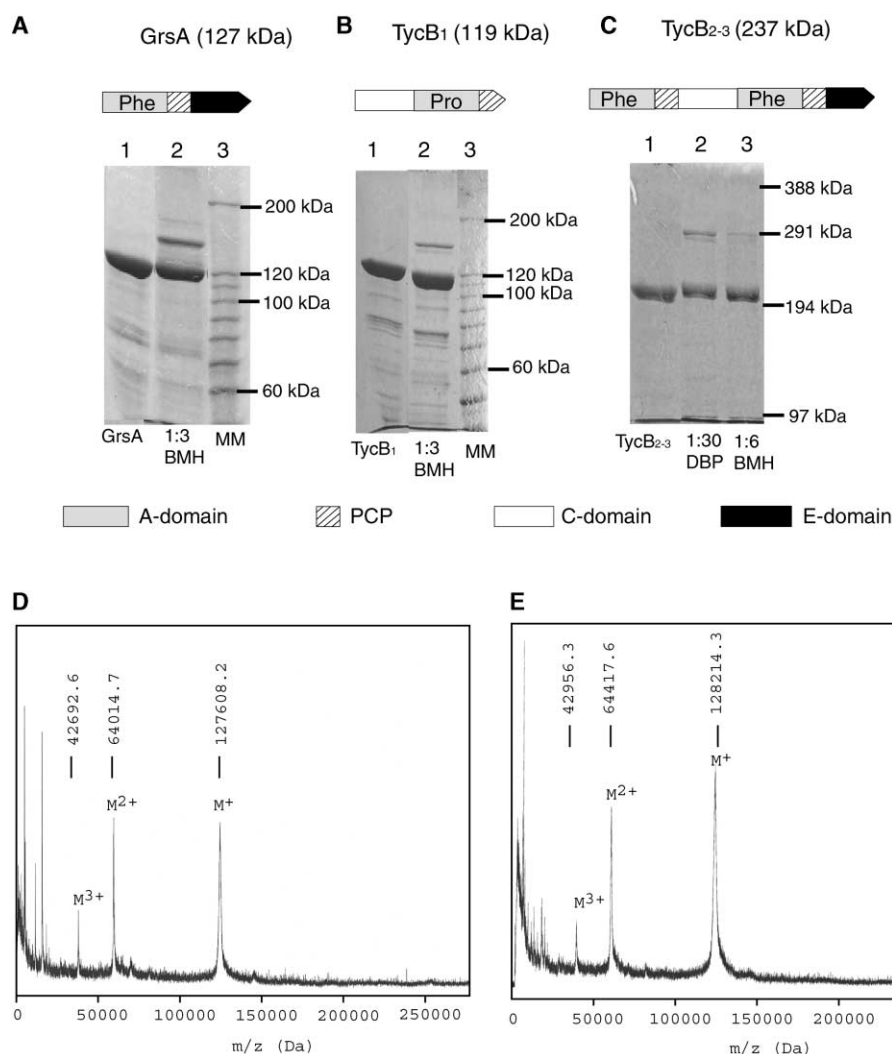
C TycB₂₋₃ (237 kDa)

Figure 2. Results of Crosslinking Experiments

(A) Polyacrylamide gel (7.5%) of GrsA (lane 1) and GrsA after incubation with a 3-fold excess of BMH (lane 2). A new protein species after incubation with BMH can be obtained corresponding to an electrophoretic mobility of ~140–160 kDa.

(B) Polyacrylamide gel (7.5%) of TycB₁ (lane 1) and TycB₁ after incubation with a 3-fold excess of BMH. Also, in the case of TycB₁ a similar shift in electrophoretic mobility from ~120 before to ~140–160 kDa after incubation with crosslinker can be observed.

(C) Polyacrylamide gel (5%) of TycB₂₋₃ (lane 1), TycB₂₋₃ after incubation with a 30-fold excess of DBP (lane 2), and after incubation with a 6-fold excess of BMH (lane 3). DBP as well as BMH lead to the formation of a new protein species corresponding to an electrophoretic mobility of ~290 kDa.

(D) MALDI-TOF mass spectra of GrsA without BMH treatment. The molecule ion peak was obtained at 127,608 Da.

(E) MALDI-TOF mass spectra of GrsA after treatment with BMH. The molecule ion peak is shifted toward a higher mass (128,214 Da) in comparison with the spectra of the untreated sample. Peaks corresponding to the masses of a dimer were not observed.

and a 0.40 O.D. loading concentration were fit to a one-component (monomer-only) model. Molecular weight was a floated global parameter and was forced to be the same for all the included data sets. The system could be well described with this monomer-only model, which resulted in random residuals (Figure 3F) and a molecular weight of 137.17 ± 8.17 kDa, which is in agreement with the protein sequence predicted molecular weight (142.97 kDa). The data fitting did not improve with a monomer-dimer model for EntF, and the experimentally fit dissociation constant (data not shown) was many orders of magnitude larger than the loading concentration. Therefore, neither gel filtration, analytical ultracen-trifugation, nor crosslinking supported a strong dimeric interaction of the investigated gramacidin, tyrocidine, and enterobactin synthetase components.

Dissociation and Reassociation of Subunits of a Putative Dimer (Scrambling)

In this study, we applied two different biochemical methods to address the quarternary structure of NRPS enzymes. Similar experiments were carried out previously to verify the dimeric structure of FAS and PKS [19, 28, 29, 31, 39]. Both methods were designed to detect het-erodimeric enzymes and give negative results for mono-meric enzymes. The critical step that is necessary for
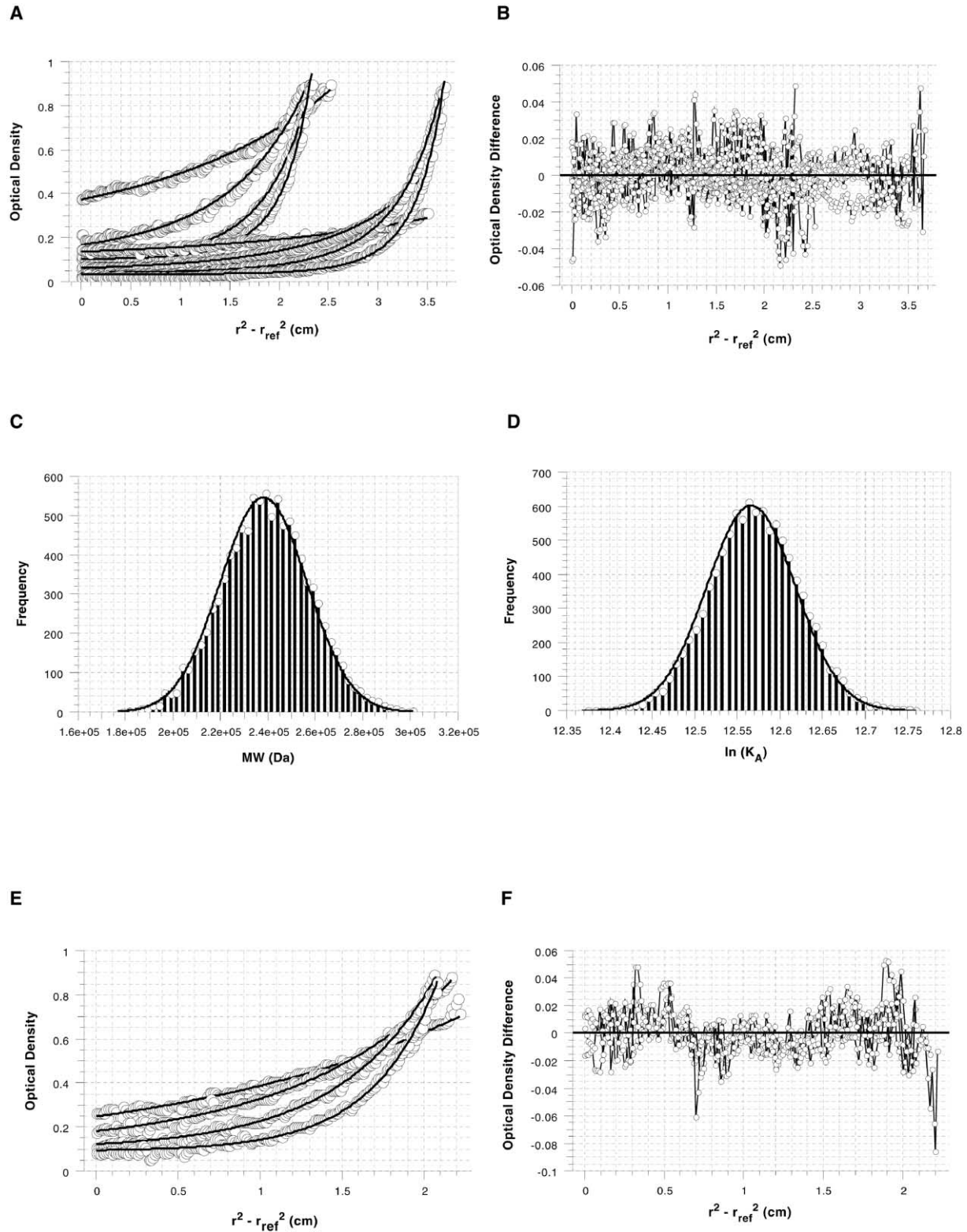
A

B

C

D

E

F

Figure 3. Sedimentation Equilibrium Analysis of TycB$_{2-3}$ and EntF

(A–D) Overlay of eight wavelength scans (A) and residuals (B) from the global fit of the data of TycB$_{2-3}$ as described in Experimental Procedures. The Monte Carlo distribution of the molecular weight (C) and the association constant (D) (ln K$_A$) are shown to establish an experimental M$_r$ = 238.07 ± 18.21 kDa (the protein sequence predicted molecular weight is 237.69 kDa) for the monomer and a dissociation constant of K$_d$ = 3.489 ± 0.186 μM for the TycB$_{2-3}$ enzyme.

(E and F) Overlay of four wavelength scans (E) and residuals (F) from the global fit of the data of EntF as described in Experimental Procedures. The Monte Carlo distribution of the molecular weight (data not shown) establishes an experimental M$_r$ = 137.17 ± 8.17 kDa for the monomer which is in agreement with the protein sequence predicted molecular weight (142.97 kDa).

both methods is the dissociation and reassociation (scrambling) of putative homodimers to form heterodimers with different affinity tags or different domain-inactivating point mutations.

Two different approaches to perform scrambling were utilized in this work. Anion exchange chromatography was applied in the same way as described previously for PKS systems [38]. Dissociation is induced by a strong interaction of putative dimer subunits with the matrix material, and reassociation can occur by increasing the salt concentration, resulting in the elution of the proteins. The aminoacylation activity of the tested enzymes did not drop after application on the anion exchange column. The aminoacylation activities before and after application to the anion exchange column of GrsA-ATE and of TycB$_{2-3}$-AT.CATE with [^{14}C]phenylalanine increased from 20% to 25% and from 60% to 65%, respectively, and that of TycB$_1$-CAT with [^{14}C]proline decreased negligibly from 15% to 13%, with all differences being in the margin of error (5%) of the method. A second approach to perform dissociation and reassociation of putative dimers was carried out with the zwitterionic detergent CHAPS. One advantage of CHAPS is its non-denaturating character which typically only directs the inhibition of protein-protein interactions, leaving the tertiary structure intact. The attachment of CHAPS molecules onto the unpolar protein residues leads to the dissociation of putative dimers and to the formation of monomers covered in micelles [40]. Subsequent dialysis induces the destruction of micelles and allows the formation of putative heterodimers. To demonstrate the favored properties of CHAPS, some preliminary experiments were implemented in this work. To allow micelle formation, CHAPS was used at a concentration of 15 mM, which is well above the critical micellar concentration. The aminoacylation activities of GrsA and TycB$_1$ with their dedicated [^{14}C]-marked amino acids did not change during and after incubation with 15 mM CHAPS, indicating a functioning tertiary structure. The aminoacylation activity of GrsA with [^{14}C]phenylalanine changed only negligibly from 15% to 17% after addition of 15 mM CHAPS and remained at 12% after dialysis. Aminoacylation activity of TycB$_1$-CAT with ^{14}C-labeled proline as substrate resulted in a minor decrease from 21% to 16% after addition of 15 mM CHAPS and remained at 20% after dialysis.

The interaction of GrsA-ATE with TycB$_1$-CAT in *trans* leads to the formation of a linear dipeptide which is cleaved by a noncatalyzed cyclization reaction, resulting in the release of D-Phe-L-Pro-diketopiperazine (DKP assay) [14]. We applied this assay to demonstrate that in the presence of 15 mM CHAPS the D-Phe-L-Pro-DKP (1,3-diketopiperazine) formation decreased by greater than 80% in comparison with the untreated sample. The in *trans* reaction between GrsA and TycB$_1$ is conducted via protein-protein interactions and was effectively inhibited by CHAPS. These two experiments showed that CHAPS interrupts protein-protein interactions for Grs and Tyc proteins and therefore has the necessary prerequisite to perform scrambling.

Two-Affinity-Tag System

The specific and reversible binding of proteins with two different affinity tags to corresponding affinity columns
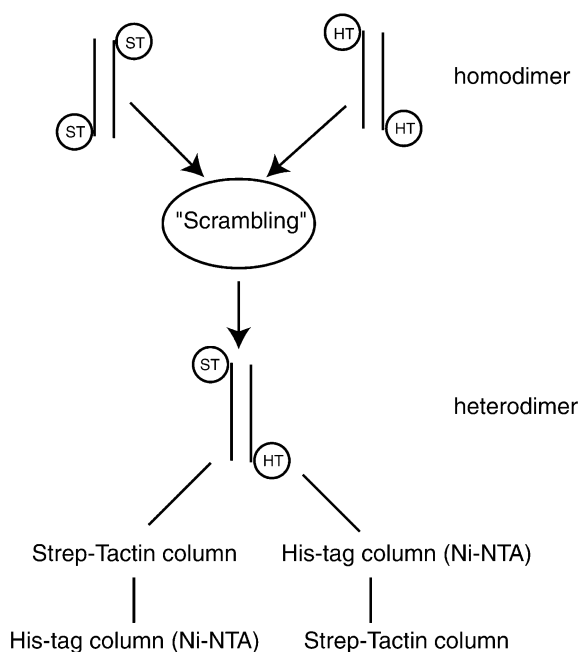

Figure 4. Heterodimer Formation with Both Strep Tag and His$_6$ Tag

Scrambling of Strep-tag and His$_6$-tag homodimers leads to the formation of heterodimers outfitted with two different affinity-tag-carrying subunits. In contrast to homodimers, these heterodimers posses the unique ability to bind to two different affinity columns, one after the other. The detection of any protein after the second column would therefore be an unequivocal proof for a dimeric behavior.

was used to test for heterodimer formation. In this experiment, two different affinity tags were utilized. Affinity chromatography on immobilized Ni ions allows the rapid purification of proteins with a fused hexahistidine-(His$_6$-) tag. The Strep tag is a small peptide with a high affinity to genetically modified streptavidin. The dimeric character of a protein can be demonstrated by scrambling of two identical homodimers which only differ in their affinity tag. The resulting heterodimer consists of two subunits with two different affinity tags. This heterodimeric protein has the unique ability to bind with its hexahistidine tag first on a Ni-NTA column and subsequently with its Strep tag on a streptavidin column or the other way around. The detection of a protein after the second column would be a proof for a dimer (Figure 4). Similar experiments with two affinity tags were carried out with dimeric FAS previously [39].

In this work, we applied both scrambling methods to conduct putative His$_6$-tag/Strep-tag heterodimer formation of GrsA and TycB$_1$, respectively. The scrambled protein samples were loaded on both affinity columns successively under conditions optimized to prevent nonspecific binding, and all elution fractions were investigated with specific hexahistidine-tag and Strep-tag antibodies. However, in all cases it was not possible to detect any protein in the elution fraction of the second column (data not shown), indicating that no heterodimers existed in solution.

Complementation

Heterodimers of fatty acid synthases and polyketide synthases carrying mutations in distinct domains are
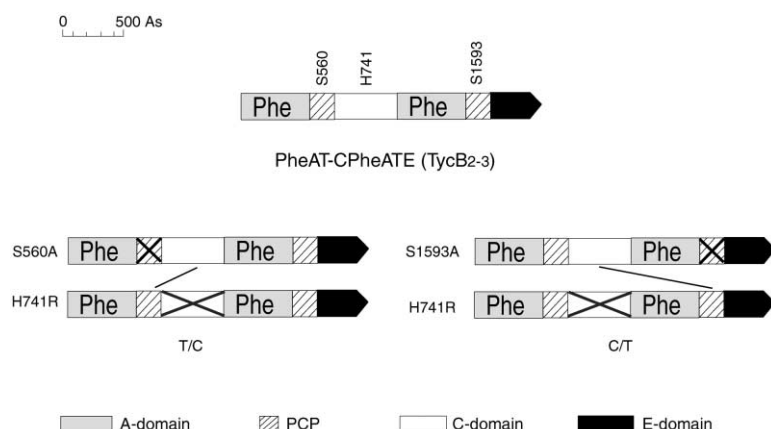
Figure 5. Complementation Systems

For the complementation assays, three different mutants of TycB$_{2-3}$ were used with mutations in the first PCP (S560A, resulting in the loss of the ability to covalently bind substrates to module one), the C domain (H741R, resulting in the breakdown of condensation activity of the enzyme), and in the second PCP (S1593A, resulting in the loss of the ability to covalently bind substrates to module two), leading to two complementation systems. The putative heterodimeric systems would either allow the interaction of the upstream PCP with the C domain or the interaction of the C domain with the downstream PCP (indicated by gray lines). In case of real heterodimers, product formation should be observed, although all three mutated enzymes show no activity by themselves.

able to balance their loss of activity by mutual complementation of the remaining active domains [19, 28, 29, 31]. The success of the mutual complementation was visualized by the ability to form product, which was a direct proof of a dimeric behavior. In this work, we tried to apply the same complementation strategy for NRPS and investigated the cooperation of PCP and C domains from TycB$_{2-3}$ after scrambling (Figure 5). Both scrambling methods were applied to conduct the formation of the putative heterodimers TycB$_{2-3(PCP)}$ (S560A)/TycB$_{2-3(C-domain)}$(H741R) and TycB$_{2-3(PCP)}$(S1593A)/ TycB$_{2-3(C-domain)}$(H741R). The phenotypes of the single mutants are the following: S560A, inactivation of the first PCP by mutation of the cofactor binding invariant serine residue, resulting in the loss of the ability to covalently bind substrates to module one; H741R, inactivation of the C domain, resulting in the breakdown of condensation activity; and S1593A, inactivation of the second PCP by mutation of the cofactor binding invariant serine residue, resulting in the loss of the ability to covalently bind substrates to module two.

Subsequently, their ability for product formation was investigated via a tripeptide assay described previously [36]. Control reactions under the same conditions were carried out using the wild-type enzyme without mutations, the mutants alone, and a mixture of both mutants without the process of scrambling. As shown in Figure 6, no product formation was observed in all experiments except in the case of the wild-type enzyme, indicating that there was no functional complementation between the enzymes inactivated in distinct domains.

Discussion

This study addressed the question of whether NRPS need a higher-order quaternary structure to function or if they work as monomers. We used several strategies that had been successfully applied to FAS and PKS systems previously and which elucidated several independent aspects of protein-protein interactions.

Results gained from gel chromatography showed a monomeric behavior of each of the NRPS enzymes. The experimental masses were slightly higher than the theoretical masses, which is likely due to the structure of the proteins differing from the ideal globular shape [41]. The results obtained from gel filtration therefore indicate a monomeric structure of NRPS which is predominantly consistent with the literature [10, 25, 32, 33, 42]. A control experiment with NRPS-PKS hybrid HMWP1 subunit of yersiniabactin synthetase revealed dimers and monomers during gel filtration, indicating an association. This shows that the method is robust enough to detect dimers and that the PKS/NRPS hybrid enzyme HMWP1 seems to be dimeric.

Analytical equilibrium ultracentrifugation is a reliable method to determine the molecular weight and detect oligomerization of solutes in the native state. Unlike gel filtration, this method is independent of calibration or shape assumptions and is therefore a good supplement to the gel filtration results.

Ultracentrifugation experiments with the PKS enzyme 6-deoxyerythronolide B synthetase 1 (DEBS1) have substantially contributed to the finding of an overall dimeric structure for PKS [20]. Analytical ultracentrifugation experiments carried out to obtain the quaternary structure of NRPS are very rare in the literature. In a sedimentation velocity analysis experiment with cyclosporin synthetase (1.4 MDa), a sedimentation coefficient of 26.3 S was observed, which led to a reasonable structural interpretation only in the case of a monomer with an oblate overall shape [42]. Here, we applied analytical equilibrium ultracentrifugation to TycB$_{2-3}$ and EntF, peptide synthetases involved in the production of a cyclic decapeptide and a siderophore, one from a gram-positive *Bacillus brevis*, one from a gram-negative *E. coli*. Results for EntF clearly indicate a monomeric structure and no aggregation at even high concentrations, which is in agreement with results from gel filtration carried out previously [32]. The dissociation constant of TycB$_{2-3}$ (3.5 μM) calculated from the ultracentrifugation data indicates oligomerization at higher nonphysiological concentrations. Assays described here were carried out at concentrations of about 0.17 μM, which would correspond to 92% monomer. Unlike dimeric PKS, these results from ultracentrifugation suggest a predominantly monomeric structure of the two investigated NRPS modules at assay and physiological concentrations.

The crosslinkers BMH and DBP differ in the length of their spacer and therefore in specificity. All three enzyme
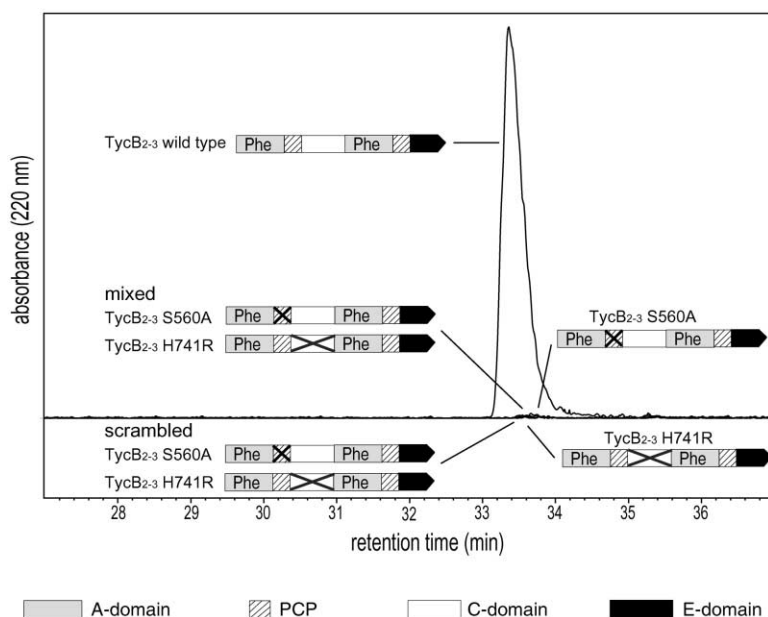
Figure 6. HPLC Trace of the Tripeptide Product-Formation Assay on the Example of the S560A/H741R TycB$_{2-3}$ Complementation System

Only the wild-type enzyme is able to produce the tripeptide. The mutated enzymes S560A and H741R did not show any detectable activity alone. Also, the mixture of S560A/H741R as well as a mixture of S1593A/H741R with and without Source Q scrambling did not exhibit any activity above background. The same results were gained for the other complementation system and scrambling method.

modules (GrsA, TycB$_1$, and TycB$_{2-3}$) reacted with BMH at low molar excess, and one new protein species with an electrophoretic mobility in between monomeric and dimeric molecular weights appeared on the SDS gel. Witkowski and coworkers already observed a similar phenomenon with crosslinked FAS [31]. They demonstrated that the new band belongs to a monomer which is intramolecular crosslinked, where altered protein shape explains the changed electrophoretic mobility of the internally crosslinked product. In consideration of the quantity of thiol groups available in the proteins (GrsA 8, TycB$_1$ 11, TycB$_{2-3}$ 13), multiple reactions with the crosslinker seem to be reasonable and support the assumption of an intramolecular linking. This finding is strongly supported by the results of MALDI-TOF mass spectrometry. The M$^+$ peaks of GrsA and TycB$_1$ were shifted to higher molecular masses, indicating the reaction of two molecules of BMH with GrsA and five molecules with TycB$_1$. Signals belonging to a dimer were not observed. In contrast to FAS and PKS, no reaction with DBP occurred with GrsA and TycB$_1$, which can be explained by the short spacer of this crosslinker. In the case of FAS, DBP was able to connect the active site cysteine of the KS domain with the closely located thiol group of the phosphopantetheine cofactor of the ACP inter- and intramolecularly [20, 31]. Such an active site cysteine does not exist in the C domain of NRPS [15], which is consistent with lack of successful DBP crosslinking in TycB$_1$, while GrsA does not have a C domain. However, the intramolecular reaction between DBP and the dimodular enzyme TycB$_{2-3}$ indicates that the flexibility of two modules may allow the approach of thiol groups into close proximity. All results gained from crosslinking did not show any dimer formation but demonstrated an intramolecular linking within a monomer.

A biochemical approach to test for oligomerization utilized a two-affinity-tag system which was adopted from investigations with FAS [39]. Neither GrsA nor TycB$_1$ demonstrated the ability to build heterodimers

containing both the Strep tag and hexahistidine tag and thereby the capacity to bind on both affinity columns successively. The specificity of the columns and of the applied antibodies were investigated and confirmed by separate experiments. Provided that the two scrambling methods were sufficient to allow dissociation and reassociation of putative dimers, the results clearly demonstrate a monomeric character of the enzymes. Complementation experiments between C and PCP domains were also adapted from previous investigations of an analogous KS and ACP complementation in FAS and PKS enzymes. The dimodular NRPS system TycB$_{2-3}$ used for these studies had the advantage to provide C-PCP interactions in *cis* compared to in *trans* in a monomodular system. None of the complementation experiments revealed any product formation, indicating that no functioning heterodimers were formed, presuming a sufficient scrambling process. Based on the results from ultracentrifugation, a maximum population of 4% heterodimers would have been possible. Product formation catalyzed by them could have been detected within the limit of the HPLC assay.

The critical step to conduct the biochemical experiments is the scrambling of homodimeric subunits to form heterodimers. Positive results would have proved unequivocally the dimeric nature of the investigated enzymes. In contrast, the negative results obtained may have two explanations: the enzymes are monomeric or the scrambling procedure was not sufficient. The zwitterionic detergent CHAPS associates with nonpolar protein residues and therefore disrupts hydrophobic interactions. The tertiary structure, at least of the A domain, is not influenced by this process, which was demonstrated by an unchanged aminoacylation activity of the enzymes (GrsA, TycB$_1$, and TycB$_{2-3}$) in presence of CHAPS and after dialysis. Furthermore, it was possible to show that CHAPS is in position to interrupt functional protein-protein interactions in *trans* between GrsA and TycB$_1$. Whether CHAPS would also be able to interrupt

protein-protein interactions in a putative NRPS dimer is speculative. The application of Source Q anion exchange chromatography was adapted from PKS experiments [38]. The principle of this method is the dissociation of proteins induced by the strong interaction with the matrix and the subsequent reassociation by an increasing salt gradient (D. Cane, personal communication). Scrambling of dimeric PKS and FAS worked very well with anion exchange chromatography.

Do NRPS Have an Oligomeric Quaternary Structure?

The related organization and chain elongation logic of PKS and NRPS as well as the existence of naturally occurring PKS-NRPS hybrids led to the assumption of a similar quaternary structure of both enzymes.

Enzymes of physiological oligomeric significance other than NRPS vary greatly in degree and strength of interaction. Examples for strongly interacting enzymes are pyruvate dehydrogenase (PDH) systems with 24-mer or 60-mer cores [43]. The complex oligomeric organization of these systems is important for the channeling of intermediates, and stiff linkers between domains of each subunit allow motion without excessive degrees of freedom [43]. In contrast to these strong interactions, FAS dimers are able to dissociate in monomers at low temperatures, whereas an equivalent behavior has never been observed for related PKS. The observed tendency of NRPS to dimerize at higher concentrations can therefore be an evolutionary relic and does not appear to have functional significance.

Crystallographic data from the PKS thioesterase domain show a hydrophobic leucine-rich dimer interface and a 2-fold symmetry axis of the dimer [44]. Such an interface has not been observed for NRPS domains based on crystallographic data [9, 24, 25], indicating that one necessary prerequisite to form dimers does not exist for NRPS.

In the case of FAS and PKS, the functional dimeric interaction takes place between the ketosynthase domains and the ACPs. Covalent intermediates can be isolated where the substrates are bound to a conserved cysteine residue of the ketosynthases, and it is mechanistically necessary that this cysteine interacts with substrates bound to the Ppant cofactors of ACPs of the second polypeptide chain of the dimer [19]. For C domains of NRPS systems, recently a reaction mechanism was suggested by the results of a mutational analysis that does not involve covalent acylenzyme intermediates [15]. There may be no such mechanistic need for NRPS to function as dimers.

In conclusion, although there is no direct experimental proof for the efficacy of the two methods for scrambling subunits between possible NRPS oligomers, the results from gel chromatography, analytical equilibrium ultracentrifugation, and crosslinking demonstrate no indication of NRPS dimers for these NRPS subunits. A monomeric structure is also supported by recent studies of cyclosporine synthetase with transmission electron microscopy, which demonstrates that nearly all 11 modules of one synthetase are not interacting with a second synthetase in a dimer [45].

Significance

Products from PKS and NRPS as well as from NRPS-PKS hybrids are biologically active compounds with an outstanding potential for new drug discovery. A prominent example is the mixed NRPS-PKS product epothilone, which is a promising candidate to combat cancer [4–6]. One goal is to improve and alter natural-product-based drugs by rational protein engineering of these enzymes (e.g., by module and domain swapping). Therefore, understanding of any oligomeric structure of these enzymes might be crucial; from investigations of PKS it is well known that the underlying reaction mechanism directly depends on the dimeric structure. Two reaction channels are open for product synthesis in a dimer. For NRPS, there was no comparable dependency of structure and mechanism known so far. The discovery of a monomeric structure of the systems investigated here closes one gap in the overall knowledge of NRPS. In particular, the observed difference in aggregation of PKS and NRPS systems is interesting with regard to the existence of hybrid enzymes. A possible structure for these hybrid enzymes could be a dimeric PKS core with monomeric NRPS loops. This structure is similar to the postulated PKS structure where optional domains are separated from the dimeric core in monomeric loops [17].

Experimental Procedures

Cloning of NRPS Fragments and Site-Directed Mutagenesis

The tyrocidine and gramicidin gene fragments corresponding to tycB$_1$ (ATTC 8185) and grsA (ATTC 9999) were amplified from chromosomal DNA by PCR using Taq and Pwo polymerase (Roche Biochemicals, Germany) with the following oligonucleotides: TycB$_1$, 5'-AAA ATA GGT CTC AAA TGA GTG TAT TT AGC AAA GAA CAA G-3' and 5'-AAA AAA GGT CTC CGC GCT TTC CAC ATA CGC TGC CAG-3'; GrsA, 5'-AAA CCG CGG GTT AAA CAG TTC TAA AAG TAT ATT GAT TC-3' and 5'-AAT ACC ATG GGT TAA TGA ATC GGC CAA ATC-3'. The PCR product tycB$_1$ was cloned into the BsaI site of the IBA3 vector, and the PCR product of grsA was cloned into the SacII/NcoI site of IBA3. The two IBA3 (IBA GmbH, Göttingen, Germany) -based plasmids direct production of the protein fragments with C-terminal Strep tag (WSHPQFEK). The cloning of pQE60 plasmids containing tycB$_{1 (35)}$, grsA [14], TycB$_{2-3}$-AT.CATE [36], and TycC$_1$-CAT/Te [36] was already described. These plasmids were directly used to produce proteins with a C-terminal His$_6$ tag.

The gene fragments encoding for the TycB$_{2-3}$ site-directed mutants S560A, H741R, and S1593A were constructed using the Quick-Change site-directed mutagenesis kit (Stratagene, Heidelberg, Germany) according to the manufacturer's protocol. All constructs were obtained by PCR amplification of the tycB$_{2-3}$ containing pQE70 plasmid [36] with the following oligonucleotides (modified sequences are underlined): S560A, 5'-GCT GGG CGG TCA TGC CTT GAA AGC GAT GAC GG-3' and 5'-CCG TCA TCG CTT TCA AGG CAT GAC CGC CCA GC-3'; H741R, 5'-CCT GTA CGA CAT GCA CCG TAT TGC TGC CGA TGC CGC-3' and 5'-GCG GCA TCG GCA ATA CGG TGC ATG TCG TAC AGG-3'; S1593A, 5'-GAA TTG GGC GG CGA TGC GAT TAA AGC GAT CCA GG-3' and 5'-CCT GGA TCG CTT TAA TCG CAT CGC CGC CCA ATT C-3'. E. coli XL1 Blue (Stratagene, Heidelberg, Germany) was used for preparation of recombinant plasmids.

Overexpression and Purification

Overproduction of recombinant hexahistidine-tagged proteins was carried out in E. coli M15 using standard protocols [46]. Purification of the hexahistidine-tagged proteins was carried out as described previously [14].

E. coli M15 cells containing the IBA3 vector were grown at 37°C before induction and at 30°C after the induction with 200 μg/l anhydrotetracycline at OD 0.6. Strep-tag-protein-containing cells were harvested by centrifugation and resuspended in buffer W (100 mM Tris-HCl [pH 8.0], 1 mM EDTA). The cells were lysed by a French press, and proteins were purified from the lysate by Strep-Tactin affinity columns (IBA GmbH, Göttingen, Germany). One milliliter of the protein-containing lysate was applied to the column, and after two washing steps with buffer W the proteins were eluted by application of 2.5 mM desthiobiotin as described by manufacturer's protocols.

After dialysis against standard assay buffer (50 mM HEPES [pH 8.0], 200 mM NaCl, 1 mM EDTA, 10 mM MgCl$_2$, 2 mM DTT), all proteins were shock frozen in liquid nitrogen and could be stored at −80°C over several months without significant loss of activity. Concentrations of the purified proteins were determined photometrically at 280 nm (mg/ml) using calculated extinction coefficients (for GrsA Strep tag, 0.89; GrsA His$_6$ tag, 0.93; TycB$_1$ Strep tag, 1.21; TycB$_1$ His$_6$ tag, 1.28; TycB$_{2-3}$, 1.05; TycC$_1$ CAT/Te, 0.97).

Activity Test and Product-Formation Assay
The A-domain activity of all enzymes (GrsA, TycB$_1$, and TycB$_{2-3}$) was tested by ATP-PP$_i$ exchange as described previously [36]. The aminoacylation activity of these enzymes was assayed by applying well-known protocols [47]. The DKP product formation assay as well as the tripeptide assay were carried out as described previously [36, 47].

Gel Filtration
Gel filtration chromatography was performed with a Sephadex 200 16/60 column as recommended by the manufacturer (Amersham Biosciences, Freiburg, Germany). The column was calibrated with apo-ferritin (443 kDa), α-mannosidase (220 kDa), lactate dehydrogenase (140 kDa), malic dehydrogenase (67 kDa), carbonic anhydrase (29 kDa), and cytochrome C (13 kDa). Each standard protein (5–10 mg) was dissolved in 1 ml standard assay buffer and loaded on the column in a 500 μl volume at 1 ml/min and eluted with the same buffer and flow rate. The detection of the proteins was carried out at 220 nm (Pharmacia FPLC-Biotechnology System 200). 1.5–2 ml of GrsA (9.0 μM), TycB$_1$ (8.5 μM), TycB$_{2-3}$ (3 μM), and HMWP1 (0.5 μM) were applied to the column in the same way as the standard proteins. In case of GrsA and TycB$_{2-3}$ in some experiments, the NaCl concentration of the standard assay buffer was increased up to 500 mM.

Analytical Ultracentrifugation
Sedimentation equilibrium experiments were performed with a Beckman Optima XL-A. Equilibrium and Monte Carlo analyses were performed with UltraScan version 5.0 [48]. Hydrodynamic corrections for buffer conditions were made according to data published by Laue et al. [49] and as implemented in UltraScan. The partial specific volumes of TycB$_{2-3}$ and EntF were estimated according to the method of Cohn and Edsall [50] and as implemented in UltraScan. TycB$_{2-3}$ samples were analyzed in a buffer containing 25 mM HEPES (pH 7) and 50 mM NaCl. EntF samples were analyzed in a buffer containing 25 mM TRIS (pH 8), 10 mM MgCl$_2$, 5 mM DTT, and 10% glycerol. Experiments were performed at 4°C at speeds ranging between 5,000 and 12,500 rpm for TycB$_{2-3}$ and between 8,000 and 17,000 for EntF. Samples were spun in a 6-channel 12 mm external fill equilibrium centerpiece in an An-60 Ti rotor. Two-hundred-eighty-nanometer scans were collected at equilibrium in radial step mode with 0.001 cm steps and 50-point averaging. Loading concentrations were 0.39 and 0.57 O.D. for TycB$_{2-3}$ and 0.40 O.D. for EntF. Data exceeding 0.9 O.D. were excluded from the fits. Data fitting was performed with a monomer-dimer equilibrium model for TycB$_{2-3}$ and with a one-component (monomer-only) model for EntF as implemented in UltraScan.

Chemical Crosslinking
Two of the three crosslinking reagents used (bismaleimidohexane [BMH] and dibromopropanone [DBP]) were dissolved in DMSO to give a final concentration of ~20 μM in the enzyme solutions (20 μl volume). The enzyme solutions did not contain DTT, which was

removed before by dialysis. The reactions were quenched with 10 mM DTT after 30 min. Dimethyl suberimidate (DMS) was dissolved in HEPES buffer (pH 7.5 and 9.5) to give a final concentration of 90 μM in the enzyme solutions (60 μl volume). Reactions were stopped after 1 hr by applying them to SDS-gel buffer. The protein samples were denatured and electrophoretically separated by using 5% and 7.5% polyacrylamide-SDS gels according to their size. The molecular masses of crosslinker-treated protein species were estimated with crosslinked phosphorylase b as a marker and additionally by MALDI-TOF mass spectrometry on a Bruker FLEX III. Protein samples for MALDI-TOF experiments were dialyzed against 0.1% TFA/water (v/v) on membranes with 0.025 μm pore diameter (Millipore, Bedford, MA) and mixed with an equal volume of saturated matrix solution (3,5-dimethoxy-4-cinnamic acid). Subsequently, 0.5 μl of this mixture was applied to the sample target plate and allowed to dry at room temperature.

Dissociation and Reassociation of a Potential Dimer (Scrambling)
Two methods were applied to dissociate and reassociate two different enzymes into potential hybrid dimers. The first method using anion-exchange chromatography on a Source Q column (Pharmacia) has been already described elsewhere [19, 38]. Additionally the zwitterionic detergent CHAPS (Biomol Feinchemikalien, Darmstadt, Germany) was utilized to reversibly dissociate putative dimers into monomers and let them reassociate after dialysis. Protein samples with a final concentration of 15 mM CHAPS were incubated for 2 hr at room temperature and afterwards the detergent was removed by a three times dialysis with standard assay buffer.

Two-Affinity-Tag System and Antibody Detection of the Enzymes
Small amounts of scrambled protein mixtures containing the same proteins with His$_6$ tag as well as Strep tag or, alternatively, the eluate of a Strep-Tactin column (see below) were applied to Ni-NTA quick spin columns (Qiagen, Hilden, Germany) according to the manufacturer's instructions. Better yields of purified proteins were gained by repeated application of the flowthrough on the column. To inhibit nonspecific binding, 50 mM imidazole was applied together with the protein sample on the column. The Strep-Tactin columns were handled as described above for protein purification. Instead of the cell lysate, the previously scrambled protein mixtures or, alternatively, the eluate of a Ni-NTA column was applied.

The hexahistidine-tagged proteins were blotted on a nitrocellulose membrane and incubated with buffer A (50 mM Tris-HCl [pH 7.5], 50 mM NaCl) containing 5% BSA overnight. The membrane was then transferred into the first monoclonal anti-His antibody (1:500) solution (mouse, IgG1, Qiagen) for 1.5 hr. After three washing steps with buffer A, the membrane was incubated for 1 hr with alkaline phosphatase-conjugated goat anti-mouse solution (DAKO, Glostrup, Denmark) in a 1:500 dilution. After washing with buffer A, the proteins were stained with 5-bromo-4-chloro-3-indolyl-phosphatate (BCIP, Promega, Madison, WI) according to the manufacturer's protocol. Strep-tag proteins were detected with the ready-to-use Strep-Tag HRP Detection Kit (IBA, Göttingen, Germany) according to the manufacturer's protocol.

References

1. Schwarzer, D., and Marahiel, M.A. (2001). Multimodular biocatalysts for natural product assembly. Naturwissenschaften *88*, 93–101.

2. Konz, D., and Marahiel, M.A. (1999). How do peptide synthetases generate structural diversity? Chem. Biol. *6*, R39–48.

3. Cane, D.E., Walsh, C.T., and Khosla, C. (1998). Harnessing the biosynthetic code: combinations, permutations, and mutations. Science *282*, 63–68.

4. Bollag, D.M., McQueney, P.A., Zhu, J., Hensens, O., Koupal, L., Liesch, J., Goetz, M., Lazarides, E., and Woods, C.M. (1995). Epothilones, a new class of microtubule-stabilizing agents with a taxol-like mechanism of action. Cancer Res. *55*, 2325–2333.

5. Molnar, I., Schupp, T., Ono, M., Zirkle, R., Milnamow, M., Nowak-Thompson, B., Engel, N., Toupet, C., Stratmann, A., Cyr, D.D., et al. (2000). The biosynthetic gene cluster for the microtubule-stabilizing agents epothilones A and B from Sorangium cellulosum So ce90. Chem. Biol. *7*, 97–109.

6. Tang, L., Shah, S., Chung, L., Carney, J., Katz, L., Khosla, C., and Julien, B. (2000). Cloning and heterologous expression of the epothilone gene cluster. Science *287*, 640–642.

7. Mootz, H.D., and Marahiel, M.A. (1999). Design and application of multimodular peptide synthetases. Curr. Opin. Biotechnol. *10*, 341–348.

8. Stachelhaus, T., Mootz, H.D., and Marahiel, M.A. (1999). The specificity-conferring code of adenylation domains in nonribosomal peptide synthetases. Chem. Biol. *6*, 493–505.

9. Conti, E., Stachelhaus, T., Marahiel, M.A., and Brick, P. (1997). Structural basis for the activation of phenylalanine in the nonribosomal biosynthesis of gramicidin S. EMBO J. *16*, 4174–4183.

10. Weber, T., Baumgartner, R., Renner, C., Marahiel, M.A., and Holak, T.A. (2000). Solution structure of PCP, a prototype for the peptidyl carrier domains of modular peptide synthetases. Struct. Fold. Des. *8*, 407–418.

11. Stachelhaus, T., and Walsh, C.T. (2000). Mutational analysis of the epimerization domain in the initiation module PheATE of gramicidin S synthetase. Biochemistry *39*, 5775–5787.

12. Burmester, J., Haese, A., and Zocher, R. (1995). Highly conserved N-methyltransferases as an integral part of peptide synthetases. Biochem. Mol. Biol. Int. *37*, 201–207.

13. Gehring, A.M., Mori, I., Perry, R.D., and Walsh, C.T. (1998). The nonribosomal peptide synthetase HMWP2 forms a thiazoline ring during biogenesis of yersiniabactin, an iron-chelating virulence factor of Yersinia pestis. Biochemistry *37*, 11637–11650.

14. Stachelhaus, T., Mootz, H.D., Bergendahl, V., and Marahiel, M.A. (1998). Peptide bond formation in nonribosomal peptide biosynthesis. Catalytic role of the condensation domain. J. Biol. Chem. *273*, 22773–22781.

15. Bergendahl, V., Linne, U., and Marahiel, M.A. (2002). Mutational analysis of the C-domain in nonribosomal peptide synthesis. Eur. J. Biochem. *269*, 620–629.

16. Kohli, R.M., Trauger, J.W., Schwarzer, D., Marahiel, M.A., and Walsh, C.T. (2001). Generality of peptide cyclization catalyzed by isolated thioesterase domains of nonribosomal peptide synthetases. Biochemistry *40*, 7099–7108.

17. Cane, D.E., and Walsh, C.T. (1999). The parallel and convergent universes of polyketide synthases and nonribosomal peptide synthetases. Chem. Biol. *6*, R319–R325.

18. Witkowski, A., Joshi, A., and Smith, S. (1996). Fatty acid synthase: in vitro complementation of inactive mutants. Biochemistry *35*, 10569–10575.

19. Kao, C.M., Pieper, R., Cane, D.E., and Khosla, C. (1996). Evidence for two catalytically independent clusters of active sites in a functional modular polyketide synthase. Biochemistry *35*, 12363–12368.

20. Staunton, J., Caffrey, P., Aparicio, J.F., Roberts, G.A., Bethell, S.S., and Leadlay, P.F. (1996). Evidence for a double-helical structure for modular polyketide synthases. Nat. Struct. Biol. *3*, 188–192.

21. Silakowski, B., Schairer, H.U., Ehret, H., Kunze, B., Weinig, S., Nordsiek, G., Brandt, P., Blocker, H., Hofle, G., Beyer, S., et al. (1999). New lessons for combinatorial biosynthesis from myxobacteria. The myxothiazol biosynthetic gene cluster of Stigmatella aurantiaca DW4/3-1. J. Biol. Chem. *274*, 37391–37399.

22. Quadri, L.E., Sello, J., Keating, T.A., Weinreb, P.H., and Walsh, C.T. (1998). Identification of a Mycobacterium tuberculosis gene cluster encoding the biosynthetic enzymes for assembly of the virulence-conferring siderophore mycobactin. Chem. Biol. *5*, 631–645.

23. Pelludat, C., Rakin, A., Jacobi, C., Schubert, S., and Heesemann, J. (1998). The yersiniabactin biosynthetic gene cluster of Yersinia enterocolitica: organization and siderophore-dependent regulation. J. Bacteriol. *180*, 538–546.

24. Weber, T., and Marahiel, M.A. (2001). Exploring the domain structure of modular nonribosomal peptide synthetases. Structure (Camb) *9*, R3–9.

25. Bruner, S.D., Weber, T., Kohli, R.M., Schwarzer, D., Marahiel, M.A., Walsh, C.T., and Stubbs, M.T. (2002). Structural basis for the cyclization of the lipopeptide antibiotic surfactin by the thioesterase domain SrfTE. Structure (Camb) *10*, 301–310.

26. Stoops, J.K., and Wakil, S.J. (1981). Animal fatty acid synthetase. A novel arrangement of the beta-ketoacyl synthetase sites comprising domains of the two subunits. J. Biol. Chem. *256*, 5128–5133.

27. Stoops, J.K., and Wakil, S.J. (1982). Animal fatty acid synthetase. Identification of the residues comprising the novel arrangement of the beta-ketoacyl synthetase site and their role in its cold inactivation. J. Biol. Chem. *257*, 3230–3235.

28. Joshi, A.K., Witkowski, A., and Smith, S. (1997). Mapping of functional interactions between domains of the animal fatty acid synthase by mutant complementation in vitro. Biochemistry *36*, 2316–2322.

29. Gokhale, R.S., Lau, J., Cane, D.E., and Khosla, C. (1998). Functional orientation of the acyltransferase domain in a module of the erythromycin polyketide synthase. Biochemistry *37*, 2524–2528.

30. Rangan, V.S., Joshi, A.K., and Smith, S. (1998). Fatty acid synthase dimers containing catalytically active beta-ketoacyl synthase or malonyl/acetyltransferase domains in only one subunit can support fatty acid synthesis at the acyl carrier protein domains of both subunits. J. Biol. Chem. *273*, 34949–34953.

31. Witkowski, A., Joshi, A.K., Rangan, V.S., Falick, A.M., Witkowska, H.E., and Smith, S. (1999). Dibromopropanone cross-linking of the phosphopantetheine and active-site cysteine thiols of the animal fatty acid synthase can occur both inter- and intrasubunit. Reevaluation of the side-by-side, antiparallel subunit model. J. Biol. Chem. *274*, 11557–11563.

32. Gehring, A.M., Mori, I., and Walsh, C.T. (1998). Reconstitution and characterization of the Escherichia coli enterobactin synthetase from EntB, EntE, and EntF. Biochemistry *37*, 2648–2659.

33. Schwecke, T., Aharonowitz, Y., Palissa, H., von Dohren, H., Kleinkauf, H., and van Liempt, H. (1992). Enzymatic characterisation of the multifunctional enzyme delta-(L-alpha-aminoadipyl)-L-cysteinyl-D-valine synthetase from Streptomyces clavuligerus. Eur. J. Biochem. *205*, 687–694.

34. Konig, A., Schwecke, T., Molnar, I., Bohm, G.A., Lowden, P.A., Staunton, J., and Leadlay, P.F. (1997). The pipecolate-incorporating enzyme for the biosynthesis of the immunosuppressant rapamycin: nucleotide sequence analysis, disruption and heterologous expression of rapP from Streptomyces hygroscopicus. Eur. J. Biochem. *247*, 526–534.

35. Mootz, H.D., Schwarzer, D., and Marahiel, M.A. (2000). Construction of hybrid peptide synthetases by module and domain fusions. Proc. Natl. Acad. Sci. USA *97*, 5848–5853.

36. Linne, U., and Marahiel, M.A. (2000). Control of directionality in nonribosomal peptide synthesis: role of the condensation domain in preventing misinitiation and timing of epimerization. Biochemistry *39*, 10439–10447.

37. Rusnak, F., Sakaitani, M., Drueckhammer, D., Reichert, J., and Walsh, C.T. (1991). Biosynthesis of the Escherichia coli siderophore enterobactin: sequence of the entF gene, expression and purification of EntF, and analysis of covalent phosphopantetheine. Biochemistry *30*, 2916–2927.

38. Pieper, R., Gokhale, R.S., Luo, G., Cane, D.E., and Khosla, C. (1997). Purification and characterization of bimodular and tri-

modular derivatives of the erythromycin polyketide synthase. Biochemistry *36*, 1846–1851.

39. Joshi, A.K., Rangan, V.S., and Smith, S. (1998). Differential affinity labeling of the two subunits of the homodimeric animal fatty acid synthase allows isolation of heterodimers consisting of subunits that have been independently modified. J. Biol. Chem. *273*, 4937–4943.

40. Dingley, A.J., Mackay, J.P., Chapman, B.E., Morris, M.B., Kuchel, P.W., Hambly, B.D., and King, G.F. (1995). Measuring protein self-association using pulsed-field-gradient NMR spectroscopy: application to myosin light chain 2. J. Biomol. NMR *6*, 321–328.

41. Lottspeich, F., and Zorbas, H. (1998). Bioanalytik (Heidelberg, Berlin: Spektrum Akademischer Verlag).

42. Schmidt, B., Riesner, D., Lawen, A., and Kleinkauf, H. (1992). Cyclosporin synthetase is a 1.4 MDa multienzyme polypeptide. Re- evaluation of the molecular mass of various peptide synthetases. FEBS Lett. *307*, 355–360.

43. Perham, R.N. (2000). Swinging arms and swinging domains in multifunctional enzymes: catalytic machines for multistep reactions. Annu. Rev. Biochem. *69*, 961–1004.

44. Tsai, S.C., Miercke, L.J., Krucinski, J., Gokhale, R., Chen, J.C., Foster, P.G., Cane, D.E., Khosla, C., and Stroud, R.M. (2001). Crystal structure of the macrocycle-forming thioesterase domain of the erythromycin polyketide synthase: versatility from a unique substrate channel. Proc. Natl. Acad. Sci. USA *98*, 14808–14813.

45. Hoppert, M., Gentzsch, C., and Schorgendorfer, K. (2001). Structure and localization of cyclosporin synthetase, the key enzyme of cyclosporin biosynthesis in Tolypocladium inflatum. Arch. Microbiol. *176*, 285–293.

46. Sambrook, J., Fritsch, E.F., and Maniatis, T. (1989). Molecular Cloning: A Laboratory Manual (Cold Spring Harbor, NY: Cold Spring Harbor Laboratory Press).

47. Linne, U., Doekel, S., and Marahiel, M.A. (2001). Portability of epimerization domain and role of peptidyl carrier protein on epimerization activity in nonribosomal peptide synthetases. Biochemistry *40*, 15824–15834.

48. Lambert, L.J., Schirf, V., Demeler, B., Cadene, M., and Werner, M.H. (2001). Flipping a genetic switch by subunit exchange. EMBO J. *20*, 7149–7159.

49. Laue, T.M., Shah, B.D., Ridgeway, T.M., and Pelletier, S.L. (1992). Computer-aided interpretation of analytical sedimentation data for proteins. In Analytical Ultracentrifugation in Biochemistry and Polymer Science, S.E. Harding, A.J. Rowe, and J.C. Horton, eds. (Cambridge: Royal Society of Chemistry), pp. 90-125.

50. Cohn, E.J., and Edsall, J.T. (1943). Proteins, Amino Acids and Peptides as Ions and Dipolar Ions (New York: Reinhold).